



# Membrane permeability during pressure ulcer formation: A computational model of dynamic competition between cytoskeletal damage and repair



N. Suhas Jagannathan<sup>a</sup>, Lisa Tucker-Kellogg<sup>a,b,c,\*</sup>

<sup>a</sup> Centre for Computational Biology, and Duke-NUS Graduate Medical School Singapore, 8 College Road, Singapore

<sup>b</sup> Program in Cancer and Stem Cell Biology, Duke-NUS Graduate Medical School Singapore, 8 College Road, Singapore

<sup>c</sup> BioSystems and Micromechanics (BioSyM) Singapore-MIT Alliance for Research and Technology, 1 Create Way, Singapore

## ARTICLE INFO

### Article history:

Accepted 14 December 2015

### Keywords:

Pressure ulcer etiology  
Computational modeling  
Membrane integrity  
Reactive oxygen species (ROS)  
Pathophysiology of mechanical injury

## ABSTRACT

Pressure ulcers are debilitating wounds that arise frequently in people who have lost mobility. Mechanical stress, oxidative stress and ischemia–reperfusion injury are potential sources of damage during pressure ulcer formation, but cross-talk between these sources has rarely been investigated. In vitro experiments with mechanically-induced cell damage previously demonstrated that non-lethal amounts of static cell deformation could induce myoblast membrane permeabilization. Permeabilization, in turn, has the potential to induce oxidative stress via leakage of calcium, myoglobin or alarmins. In this work, we constructed a hypothetical causal network of cellular-scale effects resulting from deformation and permeabilization, and we investigated the theoretical sensitivity of cell death toward various parameters and pathways of the model. Simulations showed that the survival/death outcome was particularly sensitive to the speed of membrane repair. The outcome was also sensitive to whether oxidative stress could decrease the speed of membrane repair. Finally, using the assumption that apoptosis and necrosis would have opposite effects on membrane leakage in dying cells, we showed that promoting apoptosis might under certain conditions have the paradoxical effect of decreasing, rather than increasing, total cell death. Our work illustrates that apoptosis may have hidden benefits at preventing spatial spread of death. More broadly, our work shows the importance of membrane repair dynamics and highlights the need for experiments to measure the effects of ischemia, apoptosis induction, and other co-occurring sources of cell stress toward the speed of membrane repair.

© 2016 Elsevier Ltd. All rights reserved.

## 1. Introduction

Pressure ulcers (PU) are painful, slow-healing wounds that develop over bony prominences during periods of prolonged immobility. Pressure ulcers can devastate the quality of life for people who have poor mobility. Skin is the most common layer for PU formation (Barczak et al., 1997; Vanderwee et al., 2007), and without proper care, pressure ulcers can worsen by expanding inward toward muscle and bone. Another category of pressure ulcer progresses from muscle outward. Deep tissue injury (DTI) occurs when prolonged mechanical force between bone and muscle causes the muscle to necrose near the bone, while the cutaneous layer remains intact. PU of muscle have been studied in vivo using methods such as MRI, ultrasound, and histology (Aoi

et al., 2009; Bosboom et al., 2003; Linder-Ganz et al., 2007; Peirce et al., 2000; Ruan et al., 1998; Stekelenburg et al., 2007; Strijkers et al., 2005). We focus primarily on PU of muscle because they are particularly severe and debilitating.

Previous work in the field of myocardial infarction demonstrated that muscle tissue can survive prolonged periods of ischemia but is more vulnerable to ischemia–reperfusion injury (IRI) (Vanden Hoek et al., 1996). Ischemia–reperfusion injury can damage cells through oxidative stress and production of free radicals, particularly mitochondrial superoxide (Liu et al., 1997; Shiva et al., 2007). Oxidative stress contributes to pressure ulcer pathophysiology (Taylor and James, 2005), but the etiology of pressure ulcers is more complex than ischemia or IRI alone. Studies using MRI to examine muscle perfusion and death during combinations of ischemia–reperfusion and mechanical pressure showed that the volume of necrosis induced by IRI alone was much smaller than the volume of necrosis induced by the same amount of IRI combined with mild but prolonged mechanical pressure (Loerakker et al., 2011; Stekelenburg et al., 2007).

\* Corresponding author at: Centre for Computational Biology, Duke-NUS Medical School, 8 College Road, Level 5, 169857, Singapore. Tel.: +65 6516 7654.

E-mail address: [Lisa.Tucker-kellogg@duke-nus.edu.sg](mailto:Lisa.Tucker-kellogg@duke-nus.edu.sg) (L. Tucker-Kellogg).

Therefore, pressure ulcers are not simply due to IRI, and the application of mechanical force is harmful, beyond its ability to induce ischemia/IRI.

Although cultured muscle cells can survive large amounts of mechanical deformation, small amounts of non-lethal deformation (3–12% tensile strain) were sufficient to induce permeability of myoblasts toward fluorescently tagged dextran molecules (Gefen et al., 2008; Leopold and Gefen, 2013; Slomka and Gefen, 2012). Mechanically-induced permeability allows efflux of intracellular factors, and it also allows influx of Calcium, due to the large gradient in muscle cells (0.05–0.1  $\mu\text{M}$  intracellularly,  $\mu\text{M}$ – $\text{mM}$  extracellularly). Although the sarcoplasmic reticulum (SR) can scavenge excess  $\text{Ca}^{2+}$ , high levels of  $\text{Ca}^{2+}$  influx cause SR stress, oxidative stress (Gissel, 2005) and activation of calpains, which are calcium-dependent, death-promoting proteases (Croall and DeMartino, 1991). Little is known about the cell stress and physiological effects caused by non-lethal strain and partial permeability.

In a variety of ischemic injuries including pressure injury (Stekelenburg et al., 2006; Stekelenburg et al., 2007) and burn (Lanier et al., 2011; Singer et al., 2011a), the immediate death of direct injury may be followed by delayed death of surrounding tissue, a phenomenon of spatial progression or secondary damage that is not yet well understood. Injury progression may be caused in part by loss of perfusion (Hirth et al., 2013), oxidative stress (Singer et al., 2011b), influx of calcium (Duncan, 1978; Gissel, 2005), efflux of alarmins (Hirth et al., 2012) or other disruptions of the environment. Efflux of alarmins means release of factors that indicate injury or trigger inflammation, for example, extracellular ATP (Killeen et al., 2013). Muscle cells have extremely high levels ( $\sim 5$  mg/g of wet weight) of myoglobin (Möller and Sylvén, 1981), a protein that can cause oxidative stress directly through pseudo-peroxidase reactions (Moore et al., 1998; Reeder and Wilson, 2005), or indirectly through release of heme or iron into the environment (Kumar and Bandyopadhyay, 2005; Solar et al., 1991). Pressure ulcers in animals caused significant release of myoglobin (Makhsous et al., 2010). In this work we will use Myoglobin (Mb) to represent any member of the class of diffusible intracellular factors that can cause oxidative stress (potentially via inflammation) if released extracellularly. Likewise, we use Calcium (Ca) to represent the class of extracellular molecules that can enter permeabilized cells to cause oxidative stress. The Ca category is very similar to the Mb category, except they have opposite direction of transport, and only extracellular factors are permitted to affect neighboring cells. In our model, we assumed that internal and external sources of oxidative stress are equivalent, because many ROS molecules (such as  $\text{H}_2\text{O}_2$ ) can be transported across the membrane (Fisher, 2009; Miller et al., 2010). Hence, our model differentiates between the Ca and Mb class of molecules in their ability to diffuse but not in the nature of the resulting stress.

While membrane permeability can cause cell stress and cell death, cell death is also able to affect membrane permeability. During apoptotic death, cellular contents are packaged into membrane-bound vesicles called apoptotic bodies, thereby blocking the release of alarmins and minimizing the inflammatory response (Kerr et al., 1995; Kroemer et al., 2009). In contrast, necrotic death causes lysis (rupture) of the cell membrane and release of cellular contents, resulting in inflammation (Edinger and Thompson, 2004; Mevorach et al., 2010). The threshold of injury required for causing apoptosis is lower than for causing necrosis, particularly in the case of oxidative stress (Hampton and Orrenius, 1997; Teramoto et al., 1999). However, apoptosis requires hours to execute (Albeck et al., 2008a, 2008b; Goldstein et al., 2000; Saraste, 1999), whereas necrotic lysis can be instantaneous. In other words, a cell that encounters increasing stress might initiate apoptosis at an early time-point, but before the apoptotic program can complete, the cell might succumb to necrosis. As a result,

induction of apoptosis can only prevent necrosis from occurring if the environment is hospitable enough for the cell to remain viable during the apoptotic delay.

When cells are damaged, they generally mount counter-measures, for example, membrane repair in response to membrane disruption. Important work in the lab of Arthur Mak (Duan et al., 2015) performed non-lethal laser ablation, and discovered that oxidative stress decreases the speed of membrane repair. In other words, oxidative stress can impair endogenous counter-measures against mechanical stress. Because such experiments are costly and labor-intensive, there is a need for theoretical work to explore the landscape of potential cross-talk relationships and to prioritize the choice of variables for future experimental studies.

In this work we study multiple stresses (mechanical force, partial permeability, Ca influx, Mb efflux, IRI) in the context of dynamic competition between damage and repair, and we address the following questions – (1) How sensitive is the total death to each of the rate parameters in the model. (2) What are the individual contributions of permeability and oxidative stress to the total death and how does feedback between the two impact the system? (3) How do the apoptosis/necrosis divide and related parameters affect the total death in the system? Our qualitative model captures roughly 7 cellular-scale processes that may contribute to muscle injury during pressure ulcer formation, and interconnects them in a causal network. Causal networks are reviewed by Tenenbaum et al. (2011). Each causal network is repeated in many cellular compartments over a 2-dimensional space. The 2-dimensional space can be subjected to user-defined mechanical deformations, and we have provided a simple finite element mesh with simulated force, to provide mechanical stimulus to the system.

Because very few experiments have yet been performed to quantify the damage and repair processes we study, we performed qualitative computational modeling, repeated many times across a range of variable parameters. This method allows us to explore regions of parameter space (e.g., combinations of stresses and responses) that affect the relevant outcomes, and to identify configurations of the system that may have interesting or non-monotonic behaviors. Understanding why different variables may have different relative influence over cell death may be useful for prioritizing future experiments.

## 2. Model

The model consists of repeating hexagonal compartments over a 2D plane. The hexagons are simplified abstractions of muscle fiber cross-sections, where each hexagon is a myotube compartment. Each compartment has a set of (scalar) state variables, such as membrane permeability. The dynamic competition between state variables is governed by ordinary differential equations (ODEs) with respect to time. The interdependence between variables and equations creates a causal network, described below. At each step of the ODE simulation, transport processes allow extracellular quantities to diffuse isotropically between adjacent compartments. We call this the biochemical section of the model.

To study the interplay between biochemical effects and mechanical effects, we require a physical strain field. Other labs have performed detailed finite element simulations for the effects of force on different anatomical regions (Cheung et al., 2005; Linder-Ganz et al., 2007; Linder-Ganz and Gefen, 2004; Makhsous et al., 2007). However, in keeping with the highly simplified nature of our model, we performed a finite element simulation with an ellipsoidal region of force applied to a uniform elastic 2D mesh [Supplementary Text 4] to obtain a measure for deformation of each compartment. We call this the mechanical section of the

model. The deformation variables appear in the ODEs, allowing deformation to influence other state variables, but other state variables to not affect the deformation.

The causal network model [Fig. 1A] includes the following steps. Mechanical stress increases membrane permeability, which causes efflux of Mb and influx of Ca. Each of Mb and Ca can contribute to oxidative stress. Calcium and Mb also have associated scavenging steps (simulated as first-order degradation). Oxidative stress also arises from reperfusion injury which is injected into the system, starting if/when mechanical stress is removed. The effects of ischemia on cell viability have been ignored because muscle cells can adapt to oxygen and nutrient deprivation for 24–48 h, whereas brief (3–4 h) ischemia followed by reperfusion can be lethal (Gawlitza et al., 2007a, 2007b; Labbe et al., 1987). This suggests that ischemia–reperfusion injury (IRI) is a more significant contribution to cell death than ischemia alone. Death can be caused by threshold levels of oxidative stress and/or permeability. Permeability and oxidative stress have associated repair processes (membrane repair and anti-oxidants). The ODEs are listed in the Section 3.

The ODEs can then be solved using a range of variable rate coefficients. Results can be visualized as in Fig. 1C. In this figure, ‘virtual’ strain was imposed on the central compartments (top panel) leading to their death (indicated in black). This resulted in Mb release around the dead cells (intensity shown in red in the inter-cell spaces) that could cause oxidative stress in surrounding cells (intensity shown in blue).

### 3. Methods

#### 3.1. Kinetic modeling

A set of ODEs was constructed to simulate the dynamics of injury propagation. Initial deformation values were obtained from FEM strain fields and were maintained at this constant value until the source of mechanical stress was removed, after which the deformation was removed (via exponential decay). The change in permeability was assumed to be a function of deformation and membrane repair rate. The rates for Calcium and Myoglobin (Mb) transport across the membrane were functions of permeability and scavenging. In addition, the Mb efflux was also affected by transport from neighboring units. Oxidative stress was a function of Mb and Ca levels, counteracted by the cell’s anti-oxidant response. The effect of oxidative stress on membrane repair was assumed to obey first-order kinetics. While it is possible that permeability might also affect rate constants of many processes (such as removal of deformation) the direction of this effect is not obvious. For example, it could either be assumed that permeability would increase the rate constant for deformation removal (more fluid membrane), or decrease this rate constant (weakening of the cytoskeleton). Hence we have ignored the effect of permeability on rate constants.

The approximate ranges of individual rate coefficients were chosen empirically by starting with an initial set of small values that resulted in 0% death and then studying the sensitivity of death to individual rate coefficients. The indices of the rate coefficients in the following ODEs correspond to the numbering of the arrows in Fig. 1E.

$$\frac{d[\text{Permeability}]}{dt} = (1 - \text{death}) * \left[ (k_1 * \text{Deformation}) - \left( \frac{k_{18}}{1 + \text{RepairImpairment}} \right) * \text{Permeability} \right]$$

$$\frac{d[\text{Deformation}]}{dt} = k_{\text{compression}} - \text{removal} * \text{Deformation}$$

$$\frac{d[\text{Calcium}]}{dt} = k_5 * \text{Permeability} - k_6 * \text{Calcium}$$

$$\frac{d[\text{Myoglobin}]}{dt} = k_2 * \text{Permeability} - k_3 * \text{Myoglobin} + k_{21} * \text{Myoglobin}_{\text{neighbors}}$$

$$\frac{d[\text{Oxid.Stress}]}{dt} = k_4 * \text{Myoglobin} + k_7 * \text{Calcium} + k_9 + k_{20} * \text{Oxid.stress}_{\text{neighbors}} - k_{19} * \text{Oxid.Stress}$$

$$\frac{d[\text{RepairImpairment}]}{dt} = k_{12} * \text{Oxid.Stress} + k_{17} - k_{\text{rectify\_impaired\_repair}} * \text{RepairImpairment}$$

Death was defined to be (Permeability) > Perm threshold OR (Oxidative stress) > Oxid threshold.

If either Permeability or Oxidative stress exceed their respective apoptotic threshold (which was lower than the necrotic threshold), countdown timer was begun, representing apoptotic signaling prior to apoptotic death. If Permeability or Oxidative stress exceeded their respective necrotic thresholds within the time allotted for apoptosis to complete, the cell would die by necrosis. Necrosis resulted in 100% permeability for that compartment. Apoptosis was assumed to result in 0% permeability (meaning no further influx or efflux) for that compartment. All ODEs were implemented using MATLAB.

#### 3.2. Choice of Parameters

To obtain plausible rate parameters, we compared model simulations against experimental studies of skeletal muscle death (Gawlitza et al., 2007a). Figure 7 from their study shows apoptosis and necrosis in a skeletal muscle after 20% or 40% compressive strain (Fig. 2A and B). We then varied parameters of our model so the simulations would mimic the experimental trends (Fig. 2C and D), using RMSD to measure fit. Because the model has many unknowns, the parameter values are under-determined. Nevertheless, we adopted this set of parameters as our reference model [Supplementary Table 6], because our goal is to explore qualitative trends rather than absolute quantification.

## 4. Results

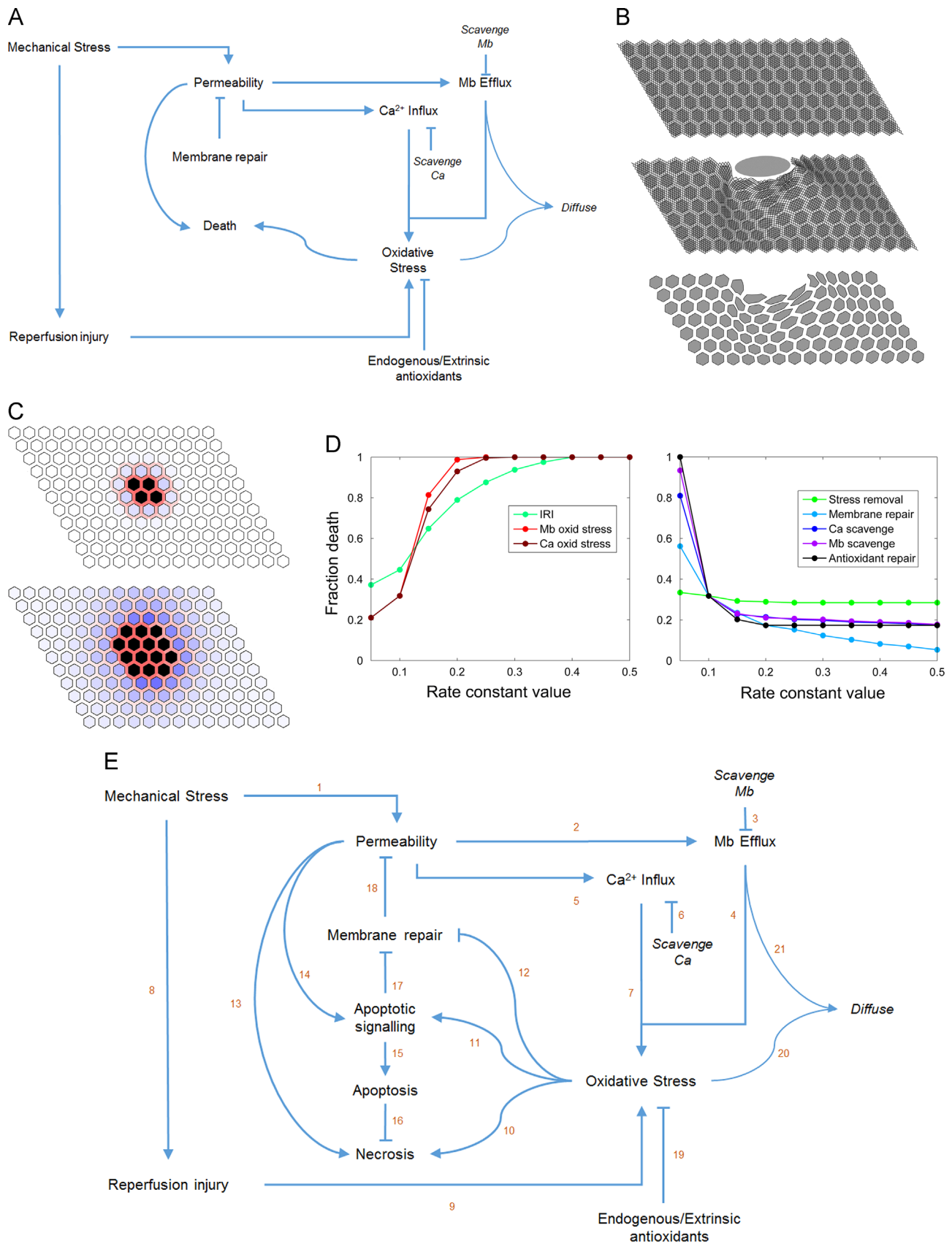
#### 4.1. Importance of repair

Fig. 1A displays the causal network used as our preliminary model. Rate coefficients were initialized to the arbitrary value of 0.1. We then performed screening simulations, varying each of the rate parameters over a range of values, to observe the relative impact of different rates toward total amount of death. Screening showed that total death was most sensitive to the rate of membrane repair (Fig. 1D). The outcome was also sensitive to the rates of Mb and Ca transport (Fig. 1D left), which affected spatial spread of injury. We also found the outcome was sensitive to the rate at which IRI induces oxidative stress (Fig. 1D left), but this finding should be tempered by the extreme simplification of IRI in the model: IRI contained no fixed time limit, so IRI was able to cause a very large effect when the simulations allowed it to occur over a long (unrealistic) period of time. We conclude that the membrane repair rate merits closer study.

In the preliminary model, repair speed was constant, but in reality repair would be affected by various forms of cell stress such as oxidative stress (Duan et al., 2015), an effect we view as “feedback” from the biochemistry toward the mechanics. We expanded the preliminary model to elaborate upon the potential regulation of membrane repair. The full model (Fig. 1E) allows oxidative stress and apoptotic signaling to impair the process of membrane repair. The full model discriminates between apoptotic and necrotic death, because during the delay between initiating and completing apoptosis, caspase enzymes digest cytoskeletal proteins such as actin, gelsolin, and focal adhesion kinase (Kothakota et al., 1997; Nicholson, 1999) and we speculate that membrane repair and cytoskeletal remodeling capacity would decrease during apoptosis. Unknown parameters were estimated (Fig. 2) as described in Section 3.

#### 4.2. Redox-mechano interplay

To study the interplay between mechanical and biochemical forms of stress, we performed simulations while removing sets of edges from the full model as shown in Table 1. To assess the impact of oxidative stress, we constructed model E1, which is identical to the full model (E0) except it lacks the ability of permeability to trigger death. E2 is identical to E1 except it also lacks



**Fig. 1.** Development of the model. (A) Simple network showing causal relationships between cellular processes during PU. Death is defined as a state that has no change in the final permeability value and results in continued transport of molecules across membrane. (B) Illustration of the finite element module used to compute deformation of cells. The panel shows the plane of hexagonal compartments with the finite element mesh overlaid (top), application of external load (middle) and the deformed plane of cells (bottom). (C) Visualization of cell states at early (top) and late (bottom) time points during an illustrative simulation. Dead cells are shown in black, the amount of myoglobin efflux is displayed in the intercellular space in red, and the amount of oxidative stress is shown in blue. (D) Early simulations indicating the sensitivity of death to the rate parameters. The panels on the left and right show the sensitivity of death to pro-death and anti-death parameters, respectively. Mb efflux and Mb contribution toward oxidative stress proved to be the most damaging, while membrane repair proved to be the most effective at promoting survival. (E) Full model including two forms of death, plus inhibition of membrane repair by oxidative stress and apoptotic signaling. Each reaction is assigned a number which also labels its rate coefficient in the model. (For interpretation of the references to color in this figure legend, the reader is referred to the web version of this article.)

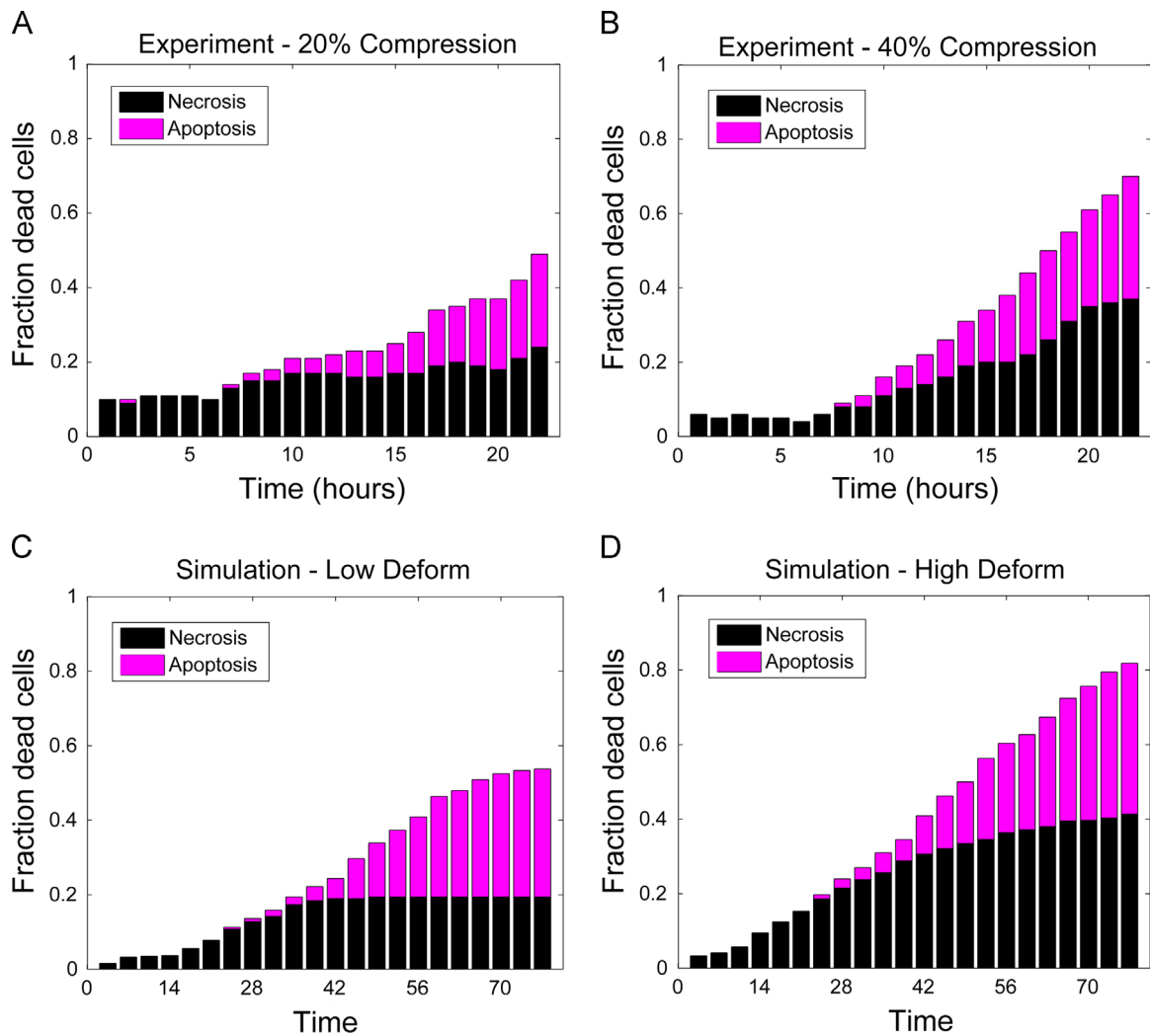


**Fig. 2.** Calibrating the model from experimental measures of apoptotic and necrotic death. (A) Percentage of necrotic and apoptotic cells in skeletal muscle subjected to 20% compression. Data obtained from Figure 7 of Gawlitta et al. (2007a) as described in Section 3. To obtain an estimate of injury-dependent death we subtracted death in unstressed control cells from the death in compressed cells. (B) Percentage of necrotic and apoptotic cells in muscle subjected to 40% compression. Data obtained as above from Figure 7 of Gawlitta et al. (2007a). (C) Percentages of apoptotic and necrotic death in our best-performing model under conditions of low deformation-induced permeability ( $k_1=4$ ). (D) Percentages of apoptotic and necrotic death in our best-performing model under conditions of high deformation-induced permeability ( $k_1=8$ ).

**Table 1**  
List of experiments performed to understand the interplay between mechanical and redox stress.

EXPERIMENT NAME	SYMBOL	REMOVED EDGES
Full model	E0	none
Death by Oxid Only	E1	13,14
Death by Oxid, No Feedback	E2	12,13,14
Death by Perm Only	E3	10,11
Death by Perm, No Efflux, No Oxid	E4	2,4,10,11,12,20,21
No Feedback	E5	12

feedback, namely the ability of oxidative stress to decrease repair. E3 was designed to assess the impact of permeability, by blocking the ability of oxidative stress to trigger death. E4 is like E3 but it also blocks all biochemical effects, including feedback, Mb efflux, and diffusion to neighboring compartments. E4 is mathematically equivalent to removing edges (2–7, 10–12, and 19–21). Model E5 is identical to the full model E0 except it lacks feedback.

For each experiment, we performed repeated simulations over a range of two pro-survival parameters: membrane repair of mechanical damage ( $k_{18}$ ), and anti-oxidant repair of biochemical damage ( $k_{19}$ ). Fig. 3A–D vary the pro-survival parameters while

comparing each of the modified models E1–E4 against the full “control” model, E0. For each comparison, we computed the difference in fraction of total death across all cells at the end of the simulation (yielding a number from 0.0 to 1.0). Fig. 3A (E0 minus E1) has near-zero differences for nearly all values of the pro-survival parameters, indicating that death was hardly affected by blocking the ability of permeability to kill cells directly. In some cases, removing the ability of permeability to contribute to death (E1) resulted in *greater* death than control (E0). This occurred because cells that would have died apoptotically in E0 (as a result of permeability) were instead dying necrotically in E1, resulting in greater environmental toxicity. Fig. 3B (E0 minus E2) resembled 3A except with higher values for the difference in total death. This indicates that feedback contributed significantly to total death for all combinations of the pro-survival parameters. Feedback was particularly important in contexts with weak anti-oxidant repair. Fig. 3C (E0 minus E3) showed that, in contexts with weak anti-oxidant response, the total amount of death was significantly affected by blocking the ability of oxidative stress to kill cells directly. Fig. 3D (E0 minus E4) shows that removing the entire biochemical section of the model caused dramatic alteration of total death, particularly for low antioxidant systems that would otherwise exhibit a high rate of death.

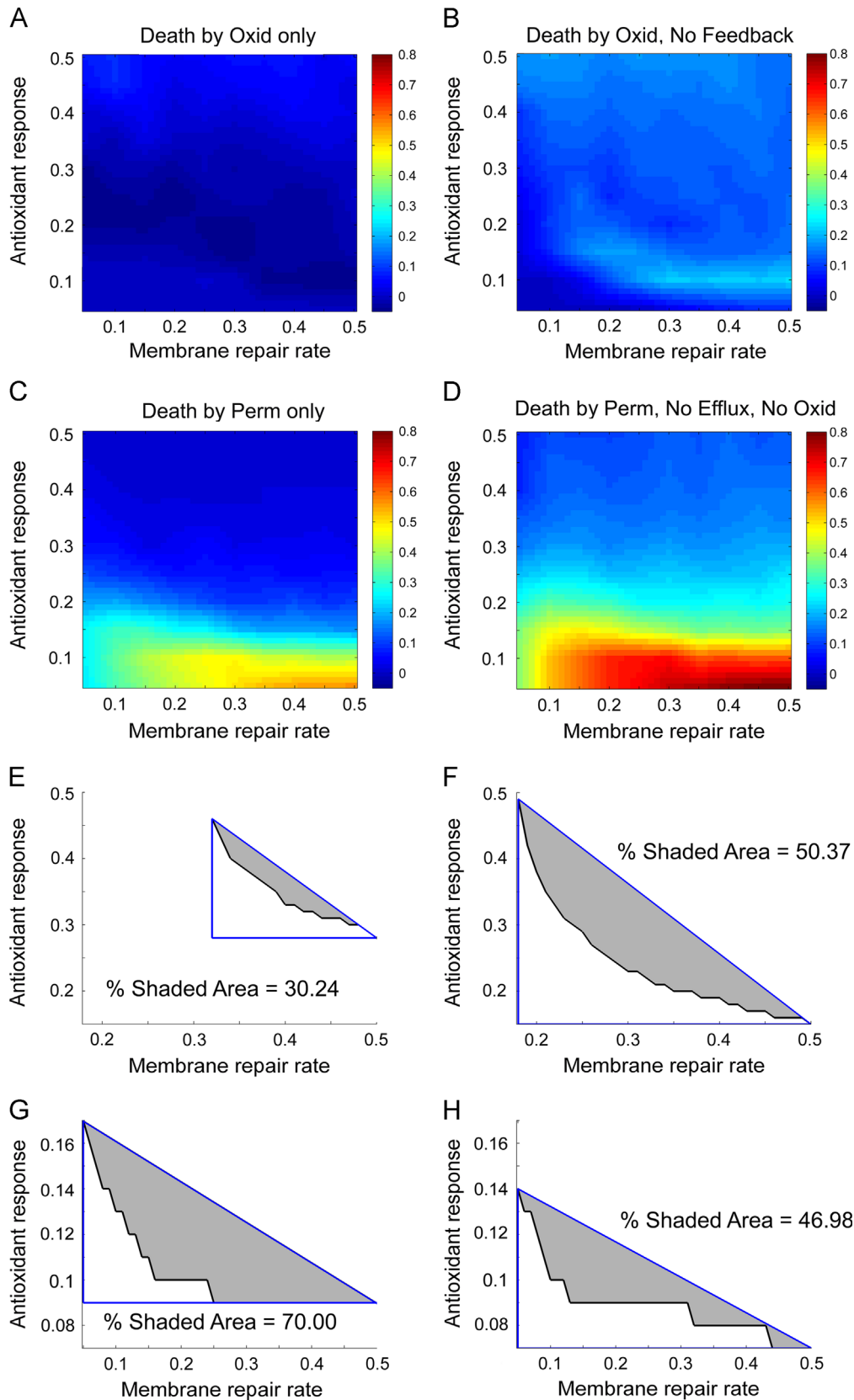


**Fig. 3.** Total death in the full model versus truncated models. See Table 1 for the naming of truncated models. (A–D) Differences between the full model (E0) and models E1–E4 in total cell death over the entire simulated region, computed for a range of values for the membrane repair rate (X-axis) and antioxidant response rate (Y-axis). Small differences in total death are shown in cooler colors and large differences are shown in warmer colors. (A) Full model versus model E1 (in which death can only be caused by oxidative stress). (B) Full model versus model E2 (in which there is no feedback and death is determined only by oxidative stress). (C) Full model versus model E3 (in which death is determined only by permeability). (D) Full model versus model E4 (which has no biochemical section). All simulations were run for 150 time steps. Membrane repair rate and antioxidant response were varied in the range [0.05–0.5], with a total of 100 simulations per model, followed by interpolation. (E) Isobologram for total death=50%, indicating the synergy between membrane repair and antioxidant response in experiment E0. (F) Isobologram for total death=50%, indicating the synergy between membrane repair and antioxidant response in experiment E5. (G and H) are the same as (E and F) except for having force=12 and  $k_1=4$ , instead of force=20 and  $k_1=8$ . In all isobologram plots, the synergy is quantified by the gray area, which is the fractional area of the triangle enclosed by the curve. (For interpretation of the references to color in this figure, the reader is referred to the web version of this article.)

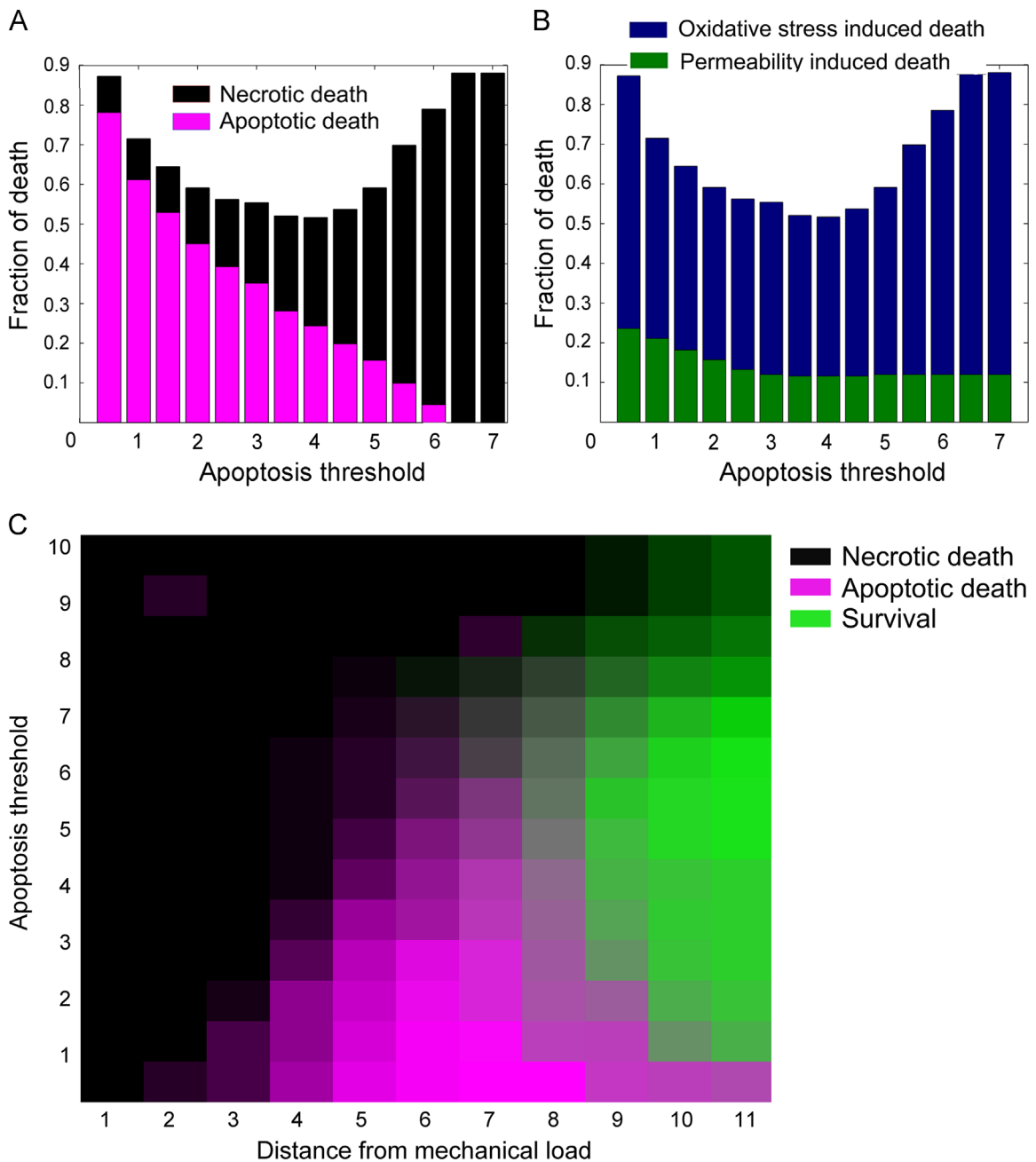
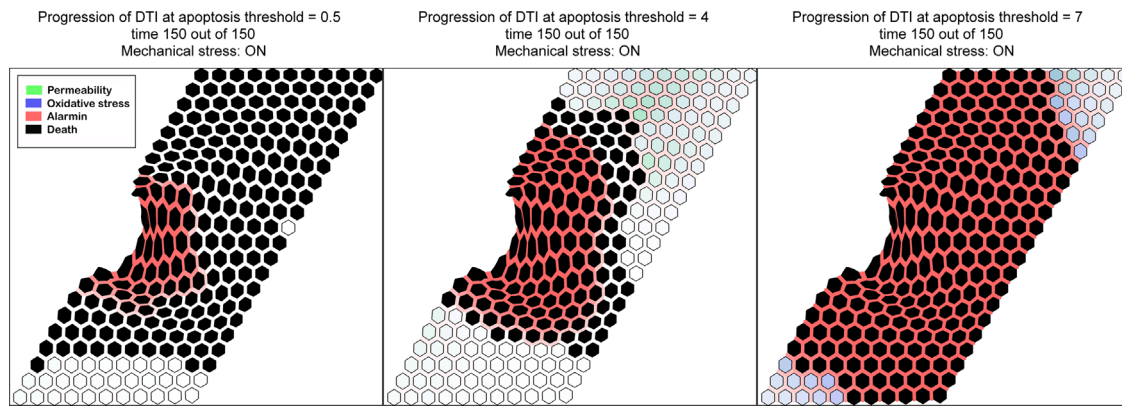


**Fig. 4.** Effect of apoptosis on fraction of death. Apoptosis threshold was varied in the range 0.5–7 in increments of 0.5 while necrotic threshold is fixed at 10. All simulations were run for 150 time steps. (A) As the apoptosis threshold is increased, the fraction of death decreases until an apoptosis threshold (4 in this case) is reached, and then increases again. Results show the proportions of necrotic death (black) and apoptotic death (magenta) in each experiment. (B) Results from the same experiment as (A) showing proportions of permeability-induced death (green) and oxidative stress-induced death (blue) in each experiment. Comparing (A) and (B) indicates that death is more oxidative-stress driven. (C) 2D phase diagram of results from same experiment as (A). The phase diagram shows regions dominated by either necrosis (black), apoptosis (magenta) or survival (green). As distance from the mechanical load increases, the fraction of apoptotic cells increases. (For interpretation of the references to color in this figure legend, the reader is referred to the web version of this article.)

The pro-survival parameters for membrane repair ( $k_{18}$ ) and anti-oxidant response ( $k_{19}$ ) are each capable of improving survival (Supplementary Fig. 1), so they might be considered for hypothetical drug therapies. To understand the additivity or synergy between these variables, we plotted isobolograms (Fig. 3E and F) for the full model (E0, left) and for the model without feedback (E5, right). Isobolograms are used in toxicology for analyzing interactions between pairs of treatments (Tallarida, 2006). In brief, isobolograms are defined by plotting all combinations of doses that cause 50% of a given downstream readout—in our case, 50% cell survival. Isobolograms display a straight line if (and only if) the two variables contribute additively. Fig. 3F and G shows that

isobolograms for our models (black lines) differ strongly from the diagonal line (blue) of an additive response, indicating strong synergism (greater-than-additive effect) from the combination of membrane repair and antioxidant response. Synergy was computed as the percentage of the shaded area in the blue triangle. The synergy of the two treatments in the full model (E0) was much less than in the model without feedback (30.24% versus 50.67%) indicating that feedback contributed to the synergy between the pro-survival mechanisms. However, when the external force and the rate of deformation-induced permeability were decreased, there was an opposite trend (Fig. 3G and H), and E0 showed higher synergy between repair mechanisms than E5.



**Video 1.** Apoptosis\_threshold\_simulation. A video clip is available online. Supplementary material related to this article can be found online at <http://dx.doi.org/10.1016/j.jbiomech.2015.12.022>.

This indicates that the impact of feedback on synergism depends on the context, and would not be robust across different parameterizations of the model. Against our expectations, treatment regimens may be able to achieve synergistic benefits, without necessarily depending on the feedback phenomenon of redox-dependent disruption of repair.

#### 4.3. Effect of death variables

Because therapeutics to inhibit apoptosis are under active research for chronic wounds such as pressure ulcers, we studied the effects of promoting or inhibiting apoptosis, by simulating networks with higher or lower thresholds for induction of apoptosis. The apoptotic threshold is the amount of damage (oxidative stress or permeability) that suffices cause initiation of apoptosis. In our simplistic model, apoptotic death occurs at a fixed time after initiation of apoptosis, unless necrotic death occurs first.

A combinatorial scan of multiple rate coefficients showed that promoting apoptosis could increase total death, as expected, but in some cases could have the indirect effect of *decreasing* total death. The left side of Fig. 4A shows that increasing the apoptotic threshold decreased the amount of apoptosis and the total amount of death, but the right side of Fig. 4A shows that further inhibition of apoptosis caused total death levels to rise, due to increased necrosis. To understand the source of increased necrosis, we separated death by whether it was triggered by oxidative stress, permeability. We found that death was dominated in all cases by oxidative stress. We believe that mechanically-induced permeability may be unavoidable in heavily loaded regions, but more distant regions (secondary damage) would depend in part on diffusible factors (such as Mb and oxidative stress) that are strongly increased by necrosis but not by apoptosis. To test whether the survival benefit of promoting apoptosis is localized to regions of secondary damage, we plotted apoptosis threshold versus distance from mechanical load [Fig. 4C]. In this scenario, central regions succumb to necrosis regardless of how apoptosis is regulated, but peripheral regions require an optimal level of apoptosis, neither too high nor too low, for maximum rate of survival (green).

## 5. Discussion

We developed a causal network model to study the interplay between mechanical and biochemical influences toward cell stress and cell death, and we provided a simple 2D framework for preliminary simulations of spatial effects and secondary damage. Using this model, we performed qualitative simulations over a

range of unitless parameter values, and we added/deleted pathways of interest. From these simulations we obtained some key insights: (1) Homeostatic processes, particularly membrane repair, could have a tremendous impact on the amount of tissue damage, and we recommend that future experiments prioritize studying loss of repair, to compensate for previous bias toward studying induction of damage. (2) Isobologram analysis showed that oxidative stress and mechanical stress were theoretically capable of great synergy, but the amount of synergy and the pathways contributing to synergy depended strongly on the context and the model parameters. Antioxidant therapies should be studied further, given the importance of antioxidant response in our simulations. (3) The contribution of apoptosis to total death was a combination of detrimental and beneficial effects. Although apoptosis can kill cells that would otherwise be viable, it also has the potential to limit permeabilization of cells that would otherwise lyse. To generalize, apoptosis is beneficial to tissue viability only when its thresholds and delays are optimally matched to occur before necrosis, and only in cells that would otherwise necrose. Therefore, therapies that target apoptosis might be most beneficial to tissue viability if they can be tailored to rectify the mismatch between apoptosis and necrosis, meaning they should allow (or promote) apoptosis in cells that are doomed to die, but not beyond. Biochemical tools exist to increase or decrease apoptotic signaling broadly, but the true challenge is to tailor the apoptotic threshold so it accurately predicts and precedes the necrotic threshold.

The qualitative results obtained from our model show *possibilities* of what might happen when underlying events occur with particular rates. In this way, the modeling is like low-resolution imaging, showing a wide scope of interest but with low precision. Future work might improve the strain computation by using a 3D FEM model and by differentiating between compaction and dilatation. In simultaneous research, our team is performing microscopy of muscle injury in fluorescent mice, an approach that provides enormous amounts of information but with narrow scope and with limited ability to perturb combinations of variables. In any scientific discipline where experimental studies require many years to provide narrow observations, theoretical research and hypothesis papers advance the scientific method by delineating patterns that might be observable, by speculating potential mechanisms for unexplained phenomena, and by simulating concrete scenarios that can fuel scientific discourse. Our computational modeling has provided such benefits by highlighting the importance of three under-appreciated factors in pressure ulcer formation: membrane repair speed, oxidative feedback toward repair speed, and the divergent effects of apoptosis and necrosis toward membrane permeability.

## Conflict of interest statement

Dr. Tucker-Kellogg has nothing to disclose.

## Acknowledgments

We would like to thank Dr. Julia Jenkins and Prof. Amit Gefen for helpful discussions. Funding for this study was provided by a block Grant from Duke-NUS, and by a special project Grant from SMART BioSyM to LT-K.

## Appendix A. Supplementary material

Supplementary data associated with this article can be found in the online version at <http://dx.doi.org/10.1016/j.jbiomech.2015.12.022>.

## References

- Albeck, J.G., Burke, J.M., Aldridge, B.B., Zhang, M., Lauffenburger, D.A., Sorger, P.K., 2008a. Quantitative analysis of pathways controlling extrinsic apoptosis in single cells. *Mol. Cell* 30, 11–25.
- Albeck, J.G., Burke, J.M., Spencer, S.L., Lauffenburger, D.A., Sorger, P.K., 2008b. Modeling a snap-action, variable-delay switch controlling extrinsic cell death. *PLoS Biol.* 6, 2831–2852.
- Aoi, N., Yoshimura, K., Kadono, T., Nakagami, G., Iizuka, S., Higashino, T., Araki, J., Koshima, I., Sanada, H., 2009. Ultrasound assessment of deep tissue injury in pressure ulcers: possible prediction of pressure ulcer progression. *Plast. Reconstr. Surg.* 124, 540–550.
- Barczak, C.A., Barnett, R.L., Childs, E.J., Bosley, L.M., 1997. Fourth national pressure ulcer prevalence survey. *Adv. Wound Care* 10, 18–26.
- Bosboom, E.M.H., Bouten, C.V.C., Oomens, C.W.J., Baaijens, F.P.T., Nicolay, K., 2003. Quantifying pressure sore-related muscle damage using high-resolution MRI. *J. Appl. Physiol.* 95, 2235–2240.
- Cheung, J.T.-M., Zhang, M., Leung, A.K.-L., Fan, Y.-B., 2005. Three-dimensional finite element analysis of the foot during standing—a material sensitivity study. *J. Biomech.* 38, 1045–1054.
- Croall, D.E., DeMartino, G.N., 1991. Calcium-activated neutral protease (calpain) system: structure, function, and regulation. *Physiol. Rev.* 71, 813–847.
- Duan, X., Chan, K.T., Lee, K.K.H., Mak, A.F.T., 2015. Oxidative stress and plasma membrane repair in single myoblasts after femtosecond laser photoporation. *Ann. Biomed. Eng.* 43 (11), 2735–2744.
- Duncan, C.J., 1978. Role of intracellular calcium in promoting muscle damage: a strategy for controlling the dystrophic condition. *Experientia* 34, 1531–1535.
- Edinger, A.L., Thompson, C.B., 2004. Death by design: apoptosis, necrosis and autophagy. *Curr. Opin. Cell Biol.* 16, 663–669.
- Fisher, A.B., 2009. Redox signaling across cell membranes. *Antioxid. Redox Signal* 11, 1349–1356.
- Gawliłta, D., Li, W., Oomens, C.W.J., Baaijens, F.P.T., Bader, D.L., Bouten, C.V.C., 2007a. The relative contributions of compression and hypoxia to development of muscle tissue damage: an in vitro study. *Ann. Biomed. Eng.* 35, 273–284.
- Gawliłta, D., Oomens, C.W.J., Bader, D.L., Baaijens, F.P.T., Bouten, C.V.C., 2007b. Temporal differences in the influence of ischemic factors and deformation on the metabolism of engineered skeletal muscle. *J. Appl. Physiol.* 103, 464–473.
- Gefen, A., Cornelissen, L.H., Gawliłta, D., Bader, D.L., Oomens, C.W.J., 2008. The free diffusion of macromolecules in tissue-engineered skeletal muscle subjected to large compression strains. *J. Biomech.* 41, 845–853.
- Gissel, H., 2005. The role of Ca<sup>2+</sup> in muscle cell damage. *Ann. N. Y. Acad. Sci.* 1066, 166–180.
- Goldstein, J.C., Kluck, R.M., Green, D.R., 2000. A single cell analysis of apoptosis. Ordering the apoptotic phenotype. *Ann. N. Y. Acad. Sci.* 926, 132–141.
- Hampton, M.B., Orrenius, S., 1997. Dual regulation of caspase activity by hydrogen peroxide: implications for apoptosis. *FEBS Lett.* 414, 552–556.
- Hirth, D.A., Singer, A.J., Clark, R.A.F., McClain, S.A., 2012. Histopathological staining of low temperature cutaneous burns: comparing biomarkers of epithelial and vascular injury reveals utility of HMGB1 and hematoxylin phloxine saffron. *Wound Repair Regen* 20, 918–927.
- Hirth, D., McClain, S.A., Singer, A.J., Clark, R.A.F., 2013. Endothelial necrosis at 1 h postburn predicts progression of tissue injury. *Wound Repair Regen* 21, 563–570.
- Kerr, J.F., Gobé, G.C., Winterford, C.M., Harmon, B.V., 1995. Anatomical methods in cell death. *Methods Cell Biol.* 46, 1–27.
- Killeen, M.E., Ferris, L., Kupetsky, E.A., Falo, L., Mathers, A.R., 2013. Signaling through purinergic receptors for ATP induces human cutaneous innate and adaptive Th17 responses: implications in the pathogenesis of psoriasis. *J. Immunol.* 190, 4324–4336.
- Kothakota, S., Azuma, T., Reinhard, C., Klippel, A., Tang, J., Chu, K., McGarry, T.J., Kirschner, M.W., Koths, K., Kwiatkowski, D.J., Williams, L.T., 1997. Caspase-3-generated fragment of gelsolin: effector of morphological change in apoptosis. *Science* 278, 294–298.
- Kroemer, G., Galluzzi, L., Vandenabeele, P., Abrams, J., Alnemri, E.S., Baehrecke, E.H., Blagosklonny, M.V., El-Deiry, W.S., Golstein, P., Green, D.R., Hengartner, M., Knight, R.A., Kumar, S., Lipton, S.A., Malorni, W., Nuñez, G., Peter, M.E., Tschoop, J., Yuan, J., Piacentini, M., Zhivotovskiy, B., Melino, G., Nomenclature Committee on Cell Death 2009, 2009. Classification of cell death: recommendations of the nomenclature committee on cell death 2009. *Cell Death Differ.* 16, 3–11.
- Kumar, S., Bandyopadhyay, U., 2005. Free heme toxicity and its detoxification systems in human. *Toxicol. Lett.* 157, 175–188.
- Labbe, R., Lindsay, T., Walker, P.M., 1987. The extent and distribution of skeletal muscle necrosis after graded periods of complete ischemia. *J. Vasc. Surg.* 6, 152–157.
- Lanier, S.T., McClain, S.A., Lin, F., Singer, A.J., Clark, R.A.F., 2011. Spatiotemporal progression of cell death in the zone of ischemia surrounding burns. *Wound Repair Regen.* 19, 622–632.
- Leopold, E., Gefen, A., 2013. Changes in permeability of the plasma membrane of myoblasts to fluorescent dyes with different molecular masses under sustained uniaxial stretching. *Med. Eng. Phys.* 35, 601–607.
- Linder-Ganz, E., Gefen, A., 2004. Mechanical compression-induced pressure sores in rat hindlimb: muscle stiffness, histology, and computational models. *J. Appl. Physiol.* 96, 2034–2049.
- Linder-Ganz, E., Shabshin, N., Itzhak, Y., Gefen, A., 2007. Assessment of mechanical conditions in sub-dermal tissues during sitting: a combined experimental-MRI and finite element approach. *J. Biomech.* 40, 1443–1454.
- Liu, P., Hock, C.E., Nagele, R., Wong, P.Y., 1997. Formation of nitric oxide, superoxide, and peroxynitrite in myocardial ischemia-reperfusion injury in rats. *Am. J. Physiol.* 272, H2327–H2336.
- Loerakker, S., Manders, E., Strijkers, G.J., Nicolay, K., Baaijens, F.P.T., Bader, D.L., Oomens, C.W.J., 2011. The effects of deformation, ischemia, and reperfusion on the development of muscle damage during prolonged loading. *J. Appl. Physiol.* 111, 1168–1177.
- Makhsous, M., Lim, D., Hendrix, R., Bankard, J., Rymer, W.Z., Lin, F., 2007. Finite element analysis for evaluation of pressure ulcer on the buttock: development and validation. *IEEE Trans. Neural Syst. Rehabil. Eng.* 15, 517–525.
- Makhsous, M., Lin, F., Pandya, A., Pandya, M.S., Chadwick, C.C., 2010. Elevation in the serum and urine concentration of injury-related molecules after the formation of deep tissue injury in a rat spinal cord injury pressure ulcer model. *PM R.* 2, 1063–1065.
- Mevorach, D., Trahtemberg, U., Krispin, A., Attalah, M., Zazoun, J., Tabib, A., Grau, A., Verbovetski-Reiner, I., 2010. What do we mean when we write “senescence,” “apoptosis,” “necrosis,” or “clearance of dying cells”? *Ann. N. Y. Acad. Sci.* 1209, 1–9.
- Miller, E.W., Dickinson, B.C., Chang, C.J., 2010. Aquaporin-3 mediates hydrogen peroxide uptake to regulate downstream intracellular signaling. *Proc. Natl. Acad. Sci. USA* 107, 15681–15686.
- Möller, P., Sylvén, C., 1981. Myoglobin in human skeletal muscle. *Scand. J. Clin. Lab. Invest.* 41, 479–482.
- Moore, K.P., Holt, S.G., Patel, R.P., Svistunenko, D.A., Zackert, W., Goodier, D., Reeder, B.J., Clozel, M., Anand, R., Cooper, C.E., Morrow, J.D., Wilson, M.T., Darley-Usmar, V., Roberts, L.J., 1998. A causative role for redox cycling of myoglobin and its inhibition by alkalization in the pathogenesis and treatment of rhabdomyolysis-induced renal failure. *J. Biol. Chem.* 273, 31731–31737.
- Nicholson, D.W., 1999. Caspase structure, proteolytic substrates, and function during apoptotic cell death. *Cell Death Differ.* 6, 1028–1042.
- Peirce, S.M., Skalak, T.C., Rodeheaver, G.T., 2000. Ischemia-reperfusion injury in chronic pressure ulcer formation: a skin model in the rat. *Wound Repair Regen.* 8, 68–76.
- Reeder, B.J., Wilson, M.T., 2005. Hemoglobin and myoglobin associated oxidative stress: from molecular mechanisms to disease states. *Curr. Med. Chem.* 12, 2741–2751.
- Ruan, C.M., Escobedo, E., Harrison, S., Goldstein, B., 1998. Magnetic resonance imaging of nonhealing pressure ulcers and myocutaneous flaps. *Arch. Phys. Med. Rehabil.* 79, 1080–1088.
- Saraste, A., 1999. Morphologic criteria and detection of apoptosis. *Herz* 24, 189–195.
- Shiva, S., Sack, M.N., Greer, J.J., Duranski, M., Ringwood, L.A., Burwell, L., Wang, X., MacArthur, P.H., Shoja, A., Raghavachari, N., Calvert, J.W., Brookes, P.S., Lefer, D. J., Gladwin, M.T., 2007. Nitrite augments tolerance to ischemia/reperfusion injury via the modulation of mitochondrial electron transfer. *J. Exp. Med.* 204, 2089–2102.
- Singer, A.J., Hirth, D., McClain, S.A., Crawford, L., Lin, F., Clark, R.A.F., 2011a. Validation of a vertical progression porcine burn model. *J. Burn. Care Res.* 32, 638–646.
- Singer, A.J., Taira, B.R., Lin, F., Lim, T., Anderson, R., McClain, S.A., Clark, R.A.F., 2011b. Curcumin reduces injury progression in a rat comb burn model. *J. Burn Care Res.* 32, 135–142.
- Slomka, N., Gefen, A., 2012. Relationship between strain levels and permeability of the plasma membrane in statically stretched myoblasts. *Ann. Biomed. Eng.* 40, 606–618.
- Solar, I., Muller-Eberhard, U., Shviro, Y., Shaklai, N., 1991. Long-term intercalation of residual heme in erythrocyte membranes distorts the cell. *Biochim. Biophys. Acta* 1062, 51–58.

- Stekelenburg, A., Oomens, C.W.J., Strijkers, G.J., Nicolay, K., Bader, D.L., 2006. Compression-induced deep tissue injury examined with magnetic resonance imaging and histology. *J. Appl. Physiol.* 100, 1946–1954.
- Stekelenburg, A., Strijkers, G.J., Parusel, H., Bader, D.L., Nicolay, K., Oomens, C.W., 2007. Role of ischemia and deformation in the onset of compression-induced deep tissue injury: MRI-based studies in a rat model. *J. Appl. Physiol.* 102, 2002–2011.
- Strijkers, G., Prompers, J., Nicolay, K., 2005. Magnetic resonance imaging and spectroscopy of pressure ulcers. In: DSc, D.L.B., Bouten, C.V.C., MD, D.C., Oomens, C.W.J. (Eds.), *Pressure Ulcer Research*. Springer, Berlin Heidelberg, pp. 317–336.
- Tallarida, R.J., 2006. An overview of drug combination analysis with isobolograms. *J. Pharmacol. Exp. Ther.* 319, 1–7.
- Taylor, R., James, T., 2005. The role of oxidative stress in the development and persistence of pressure ulcers. In: DSc, D.L.B., Bouten, C.V.C., MD, D.C., Oomens, C.W.J. (Eds.), *Pressure Ulcer Research*. Springer, Berlin Heidelberg, pp. 205–232.
- Tenenbaum, J.B., Kemp, C., Griffiths, T.L., Goodman, N.D., 2011. How to grow a mind: statistics, structure, and abstraction. *Science* 331, 1279–1285.
- Teramoto, S., Tomita, T., Matsui, H., Ohga, E., Matsuse, T., Ouchi, Y., 1999. Hydrogen peroxide-induced apoptosis and necrosis in human lung fibroblasts: protective roles of glutathione. *Jpn. J. Pharmacol.* 79, 33–40.
- Vanden Hoek, T.L., Shao, Z., Li, C., Zak, R., Schumacker, P.T., Becker, L.B., 1996. Reperfusion injury on cardiac myocytes after simulated ischemia. *Am. J. Physiol.* 270, H1334–H1341.
- Vanderwee, K., Clark, M., Dealey, C., Gunningberg, L., Defloor, T., 2007. Pressure ulcer prevalence in Europe: a pilot study. *J. Eval. Clin. Pract.* 13, 227–235.